ANGULAR DISTRIBUTIONS AND ANISOTROPY OF FISSION FRAGMENTS FROM NEUTRON-INDUCED FISSION OF ^{232}Th, ^{233}U, ^{235}U, ^{238}U, ^{239}Pu, ^{nat}Pb AND ^{209}Bi IN INTERMEDIATE ENERGY RANGE 1- 200 MEV

A.M. Gagarski[1], A.S. Vorobyev[1], O.A. Shcherbakov[1], L.A. Vaishnene[1], A.L. Barabanov[2,3]

[1]NRC "Kurchatov Institute", B.P. Konstantinov Petersburg Nuclear Physics Institute, 188300, Gatchina, Leningrad district, Russia
[2]NRC "Kurchatov Institute", 123182, Moscow, Russia
[3]Moscow Institute of Physics and Technology, 141700, Dolgoprudny, Moscow Region, Russia

Abstract

Angular distributions of fission fragments from the neutron-induced fission of ^{232}Th, ^{233}U, ^{235}U, ^{238}U, ^{239}Pu, ^{nat}Pb and ^{209}Bi have been measured in neutron energy range 1-200 MeV at the neutron TOF spectrometer GNEIS based on the spallation neutron source at 1 GeV proton synchrocyclotron of the NRC KI – PNPI (Gatchina, Russia). The multiwire proportional counters have been used as a position-sensitive fission fragment detector. A description of the experimental equipment and measurement procedure is given. The anisotropy of fission fragments deduced from the data on measured angular distributions is presented in comparison with experimental data of other authors, first of all, the recent data from LANL and CERN. The data on anisotropy and angular distributions of fission fragments in neutron energy range above 20 MeV for ^{233}U, ^{239}Pu, ^{nat}Pb and ^{209}Bi have been obtained for the first time.

1. Introduction

Neutron-induced fission cross-sections and angular distributions of fission fragments are the main sources of information about fission barrier structure and nuclear transitional states on the barrier. The relevant experimental data have been accumulated over decades, mostly for E_n < 20 MeV (E_n is the energy of incident neutrons). These data are not only of high scientific value, but of great significance for nuclear technologies as well. Nowadays, a discussion on accelerator-driven systems for nuclear power generation and nuclear transmutation has created considerable interest to nuclear fission at intermediate (E_n < 200 MeV) and higher neutron energies.

Angular distributions of fission fragments are associated with two phenomena. First, an ensemble of spins of fissioning nuclei is to be aligned and, second, distribution of transitional states over the projection K of nuclear spin on the fission axis should be non-uniform. The first factor is determined by the processes which precede to fission, while the latter one is given by the mechanism of fission. At the energies much exceeding the fission barrier, the fission is preceded by the multi-step particle emission. A relative contribution of equilibrium and non-equilibrium processes into the dynamics of highly excited nuclei is not clear up to now. The measurements of angular distributions of fragments from neutron-induced fission at the energies up to 200 MeV may shed some light on this question.

In this report, we summarize the results of the measurements carried out at the neutron time-of-flight (TOF) spectrometer GNEIS [1, 2] of the NRC KI - PNPI during the last few years. In a series of journal articles [3-5], we have reported the data on angular distributions and anisotropy of fragments from neutron-induced fission of the target nuclei ^{235}U, ^{238}U and ^{232}Th [3], ^{233}U and ^{209}Bi [4], ^{239}Pu and ^{nat}Bi [5] in the intermediate energy range 1-200 MeV. Some more details of the measurements, as well as the results, can be found elsewhere [6-10].

2. General description of the experiment

The measurements were carried out at the 36 m flight path of the neutron TOF-spectrometer GNEIS. A schematic view of the experimental set-up is shown in Fig. 1. Detailed description of the set-up and 8-input readout system based on two DC-270 Acqiris waveform digitizers can be found in our previous publications [3-10].

The targets of ^{232}Th (100 %) and ^{235}U (90 % enrichment) ~150-200 μg/cm^2 of thickness were produced by vacuum deposition of tetrafluorides of these materials on a 2 μm thick Mylar foil. The ^{233}U (82.9 %) target ~200 μg/cm^2 of thickness and ^{238}U (natural uranium) target 350 μg/cm^2 of thickness were made by painting technique with U_3O_8 deposits on a 100 μm thick Al foil. The ^{239}Pu (99.76 %) target ~300 μg/cm^2 of thickness was made using the same technique with a PuO_2 deposit. The targets of ^{nat}Pb and ^{209}Bi ~150-1000 μg/cm ^{2} of thickness were produced by vacuum deposition of high purity metal on a 2 μm thick Mylar foil.

The fission fragment registration was performed by two coordinate-sensitive multiwire proportional counters D1 and D2 (MWPC) 140x140 mm^2 of size. The fragment counters D1 and D2 were placed close to the target in the beam one after the other. The neutron beam axis came through the geometrical centers of the target and the MWPC's electrodes being perpendicular to them. In order to have a possibility to take into account for the linear momentum contribution into the measured angular distribution, the measurements with two set-up orientations relative to the beam direction (downstream and upstream) were performed.

Time and pulse-height analysis of the signal waveforms allowed to derive the neutron energy and the fission fragment coordinates on the MWPCs, and, hence, the angle information. A value of cos(θ), where θ is an angle between neutron beam axis and fission fragment momentum, can be derived easily from the coordinates of the fission fragment measured by two counters.

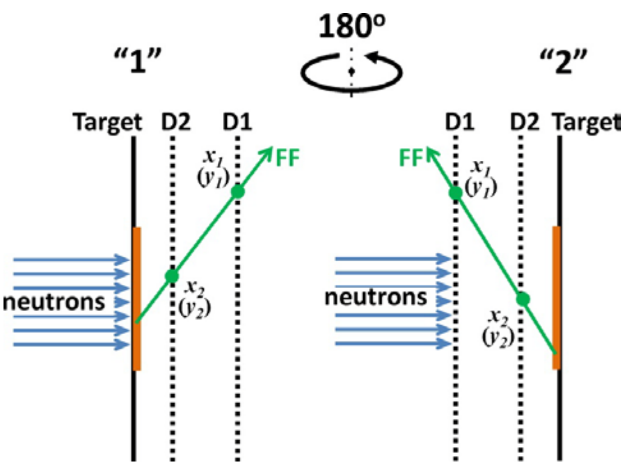

Fig. 1a. Schematic view of the experimental set-up at two orientations relative to the neutron beam direction (downstream and upstream)

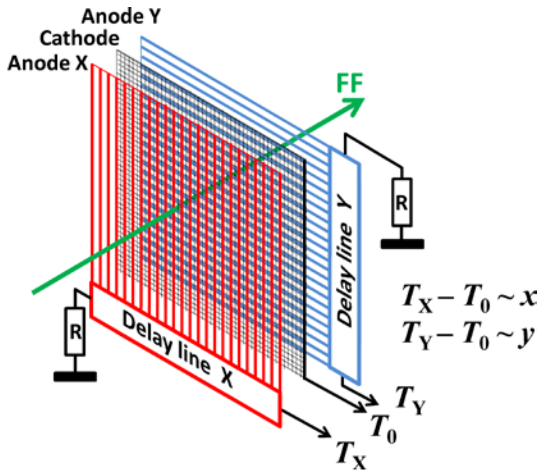

Fig. 1b. Construction of the MWPC. The coordinates are determined from the time delay of signals from anodes (T_X and T_Y) with respect to a signal from the cathode (T_0).

The measured angular distributions for selected fission fragment events were corrected for the efficiency of fission fragment registration. This efficiency was calculated by means of the Monte-Carlo method taking into account following parameters: the electrode wire structure, distances between MWPCs and target, sizes of electrodes and distances between them, sizes of the target and neutron beam, the position (angular) resolution (~2 mm). Also, the additional corrections due to the differential nonlinearity of the delay line chips and the mutual influence (signal cross-talk) of the anodes of two adjacent MWPCs were taken into account [4].

An anisotropy W(0^o)/W(90^o) of angular distributions of fission fragments in the center-of-mass system were deduced from the corrected cos(θ) angular distributions in the laboratory system for two set-up orientations relative to the neutron beam direction (cos(θ) bins were equal to 0.01) by fitting them in the range 0.24 < cos(θ) < 1.0 by the sum of even Legendre polynomials up to the 4-th order.

3. Results and discussion

Until 2000, practically all measurements [11-23] of the fission fragment angular distributions were carried out using beams of monoenergetic neutrons in energy range below 14 MeV (sometimes up to 24 MeV) at the Van-de-Graaff and Cockroft-Walton accelerators, as well as in the energy range 20-100 MeV at the cyclotron of the TSL (Uppsala) [21,24].

A new age in experimental investigations of the fission fragment angular distributions started when new experiments dedicated to this problem have been initiated nearly simultaneously by the GNEIS team at NRC KI - PNPI [3-10], the n_TOF Collaboration at CERN [25-29], and the NIFFTE Collaboration in Los Alamos [30, 31]. The pulsed high-intensity “spallation” neutron sources of these facilities enable to carry out TOF-measurements of the neutron-induced fission cross sections and fission fragment angular distributions in intermediate neutron energy range 1-300 MeV. The other two principally important features of the experimental techniques employed by these research groups are usage of the multichannel position-sensitive detectors of fission fragments of different degree of complexity (MWPCs, PPACs, TPC), and application of the wave-form digitizers for detector pulse processing.

The anisotropy W(0^o)/W(90^o) obtained at the GNEIS by fitting the fission fragment angular distributions measured for ^{232}Th, ^{233}U, ^{235}U, ^{238}U, ^{239}Pu, ^{nat}Pb and ^{209}Bi in the neutron energy range 1-200 MeV is shown in Fig. 2-8. The figures also show experimental data obtained by other authors [11-31]. It can be stated that the results obtained at the GNEIS below ~ 20 MeV adequately represent the structures in energy behavior of the anisotropy observed in early measurements, and this circumstance ensures reliability of the experimental technique employed. At present, a comparison of our results obtained in the energy range 20-200 MeV for ^{232}Th, ^{235}U and ^{238}U can be done with analogous data measured at LANL and n_TOF. Fig. 3 displays obvious disagreement between our data for ^{235}U [3] and those obtained by n_TOF (Leal-Cidoncha [28]) and LANL (Kleinrath [30]) in a whole energy range 1-200 MeV. The latest data sets presented by n_TOF [29] and LANL [31] collaborations shown in Fig. 8 significantly improved agreement with our data though their numerical data still are absent in the EXFOR data base. Large uncertainties of the ^{238}U data presented by n_TOF (Leal-Cidoncha [29]) do not allow to make an unambiguous conclusion about agreement between our data sets above ~ 20 MeV (Fig. 4), whereas data by Ryzhov [25] are definitely higher that our data above ~ 40 MeV. In a case of ^{232}Th shown in Fig. 5, one of two data sets obtained by n_TOF [25-27] agrees within experimental uncertainties with our data above ~ 20 MeV (Leong [25]), while the other (Tarrio [27]) is much higher. And again, data by Ryzhov [25] are higher than all other data sets. The observed disagreements leave a space for thorough analysis of the possible systematic errors specific for every experimental procedure used in the measurements mentioned above.

An undoubted achievement of present work is the fact that experimental data on fission fragment angular distributions above ~ 20 MeV for ^{233}U, ^{239}Pu, ^{nat}Pb and ^{209}Bi have been obtained for the first time. For ^{nat}Pb and ^{209}Bi the measurements are especially difficult because neutron-induced fission cross sections of these nuclei are 10-100 lower than those of

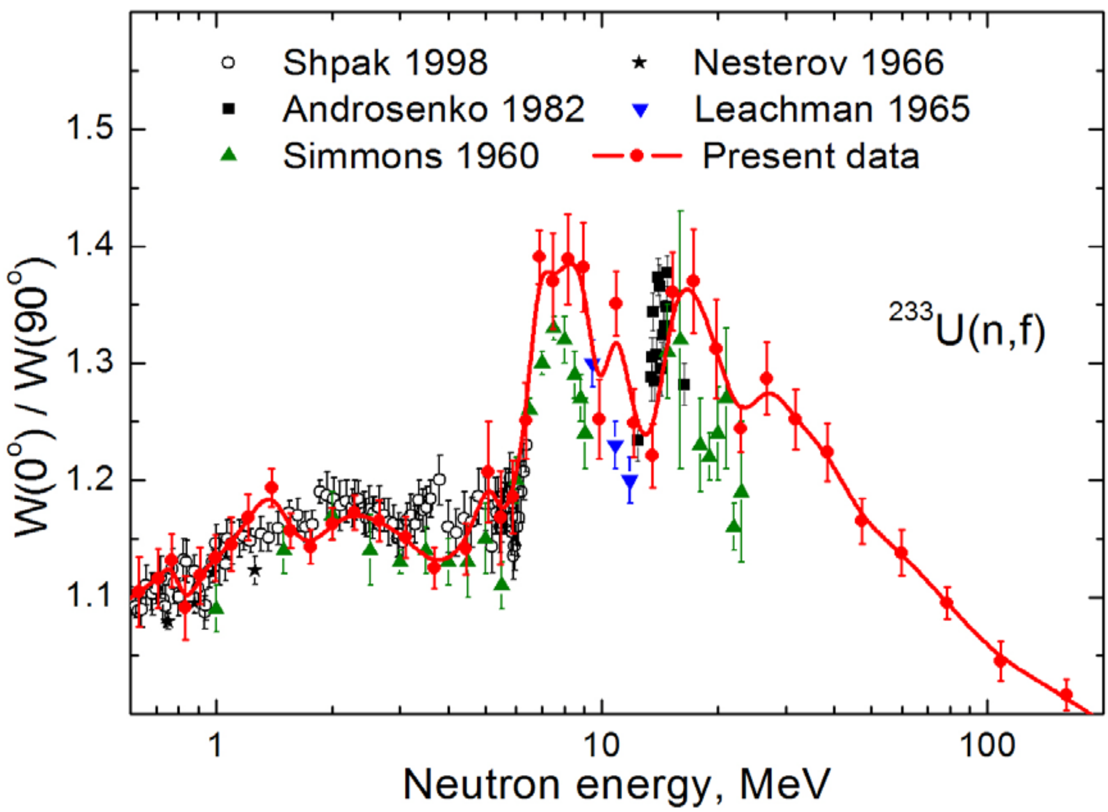

Fig. 2. Anisotropy of fission fragments of ^{233}U

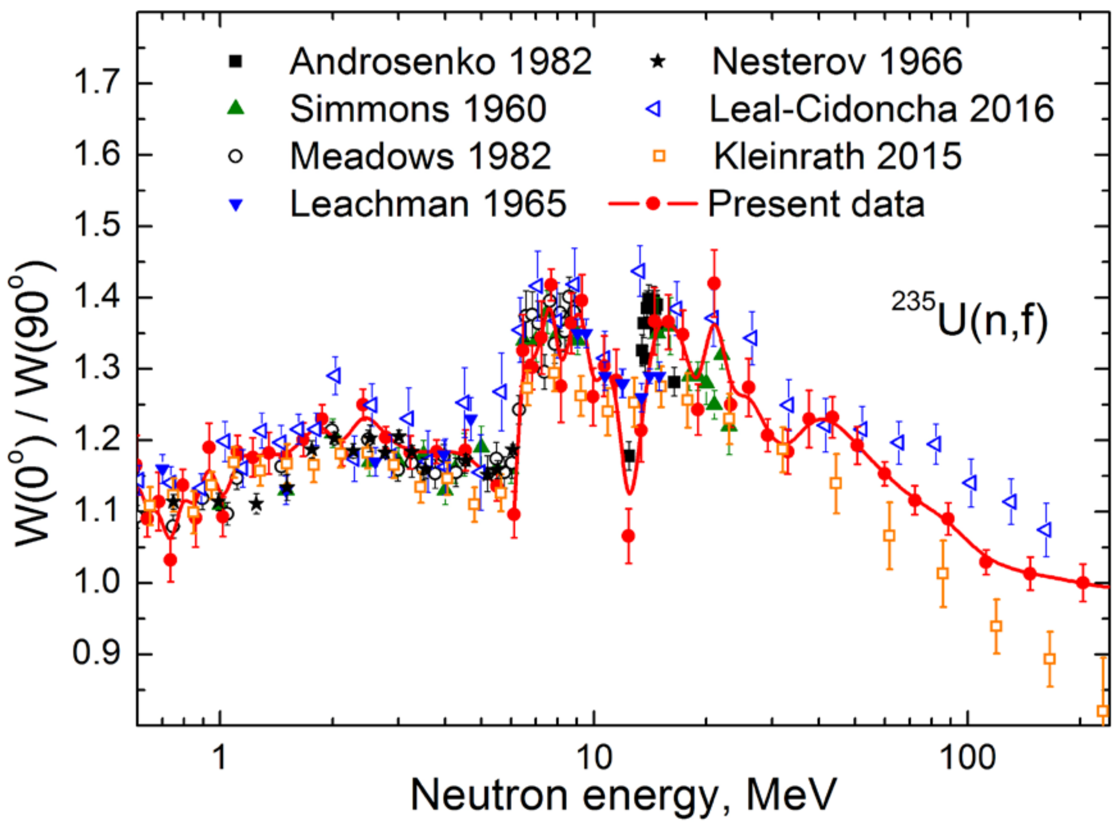

Fig. 3. Anisotropy of fission fragments of ^{235}U.

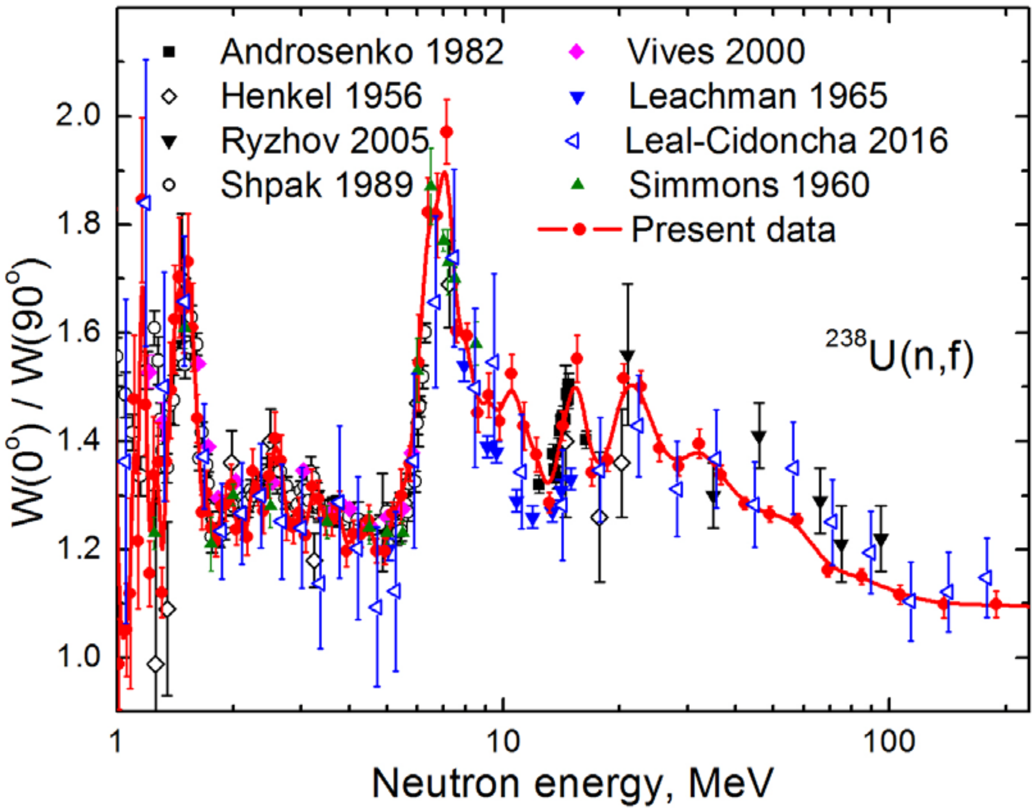

Fig. 4. Anisotropy of fission fragments of ^{238}U.

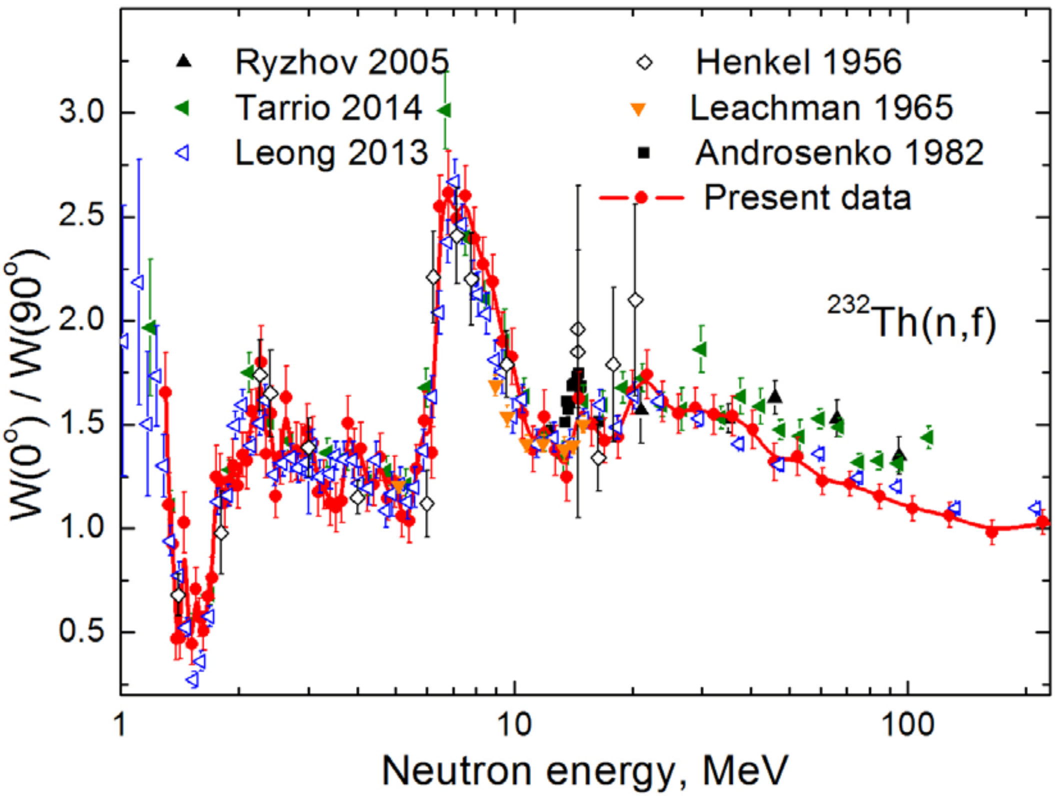

Fig. 5. Anisotropy of fission fragments of ^{232}Th.

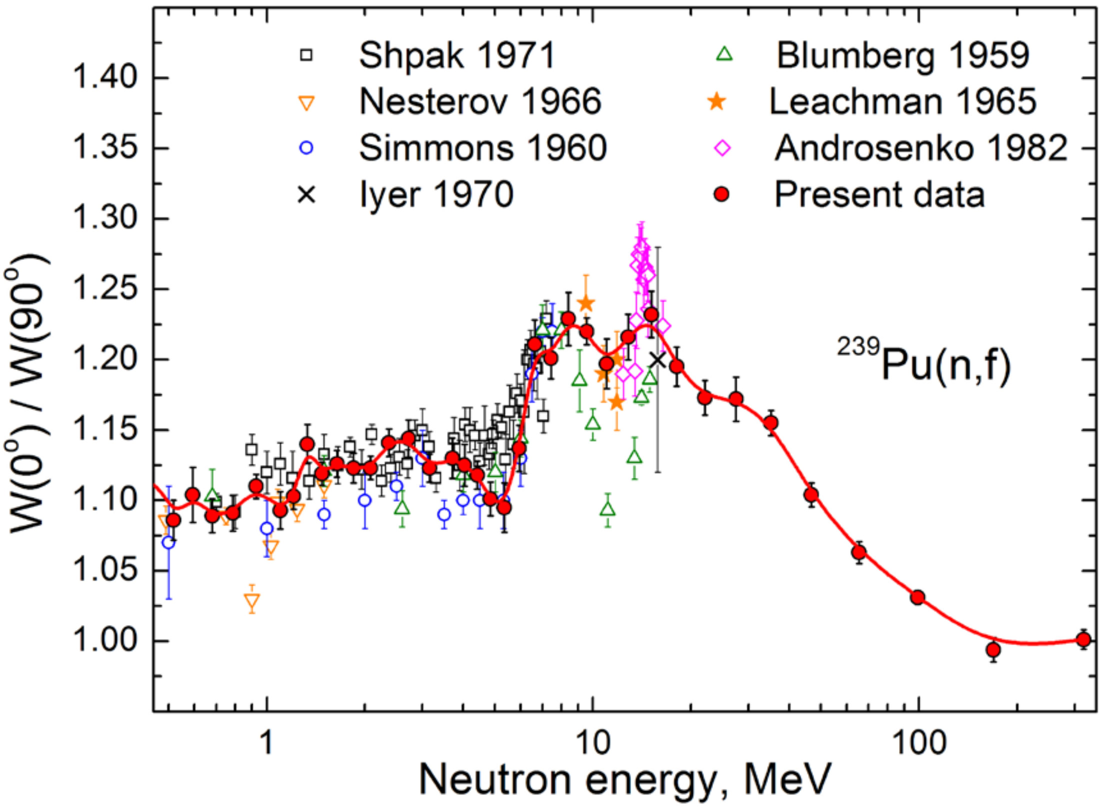

Fig. 6. Anisotropy of fission fragments of ^{239}Pu.

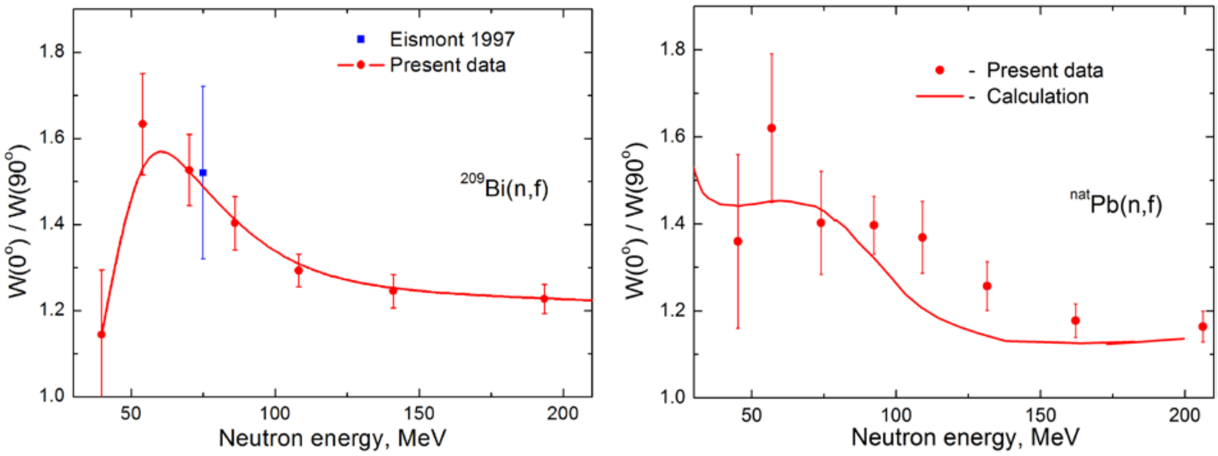

Fig. 7. Anisotropy of fission fragments of ^{209}Bi (left) and ^{nat}Pb (right)

actinides. As a consequence, background problems and low counting statistics lead to vast machine-time expenditures.

Our next goal is a measurement of the fission fragment angular distributions for ^{237}Np. The only one data set for this nucleus was obtained in neutron energy range from 0.1 MeV up to 1 GeV at the n_TOF (Leong [25]). Unfortunately, it is characterized by large error bars and, therefore, can't be treated as a completed research. An upper neutron energy range of the other (comparatively old) experimental data for ^{237}Np included in the EXFOR data base do not exceeds 15 MeV.

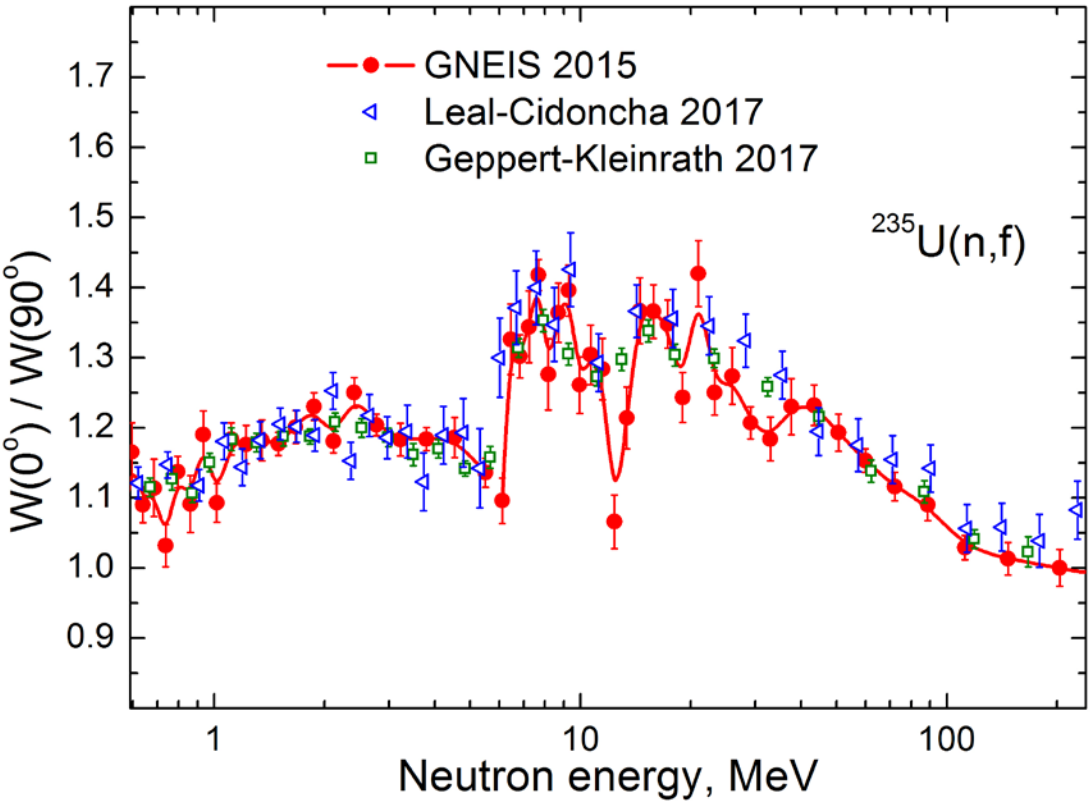

Fig. 8. Anisotropy of fission fragments of ^{235}U.

Acknowledgments

The authors would like to thank the staff of the Accelerator Department of the NRC KI - PNPI for their permanent friendly assistance and smooth operation of the synchrocyclotron during the experiment and T.E. Kuz'mina (Khlopin Radium Institute, St. Petersburg, Russia) for cooperation in the preparation of high-quality actinide targets. This work was supported in part by the Russian Foundation for Basic Research (Project no. 18-02-00571).

References

[1] N.K. Abrosimov, G.Z. Borukhovich, A.B. Laptev, V.V. Marchenkov, G.A. Petrov, O.A. Shcherbakov, Yu.V. Tuboltsev, and V.I. Yurchenko, Nucl. Instrum. Methods Phys. Res. A **242**, 121 (1985).
[2] O.A. Shcherbakov, A.S. Vorobyev, and E.M. Ivanov, Phys. Part. Nucl. **49**, 81 (2018).
[3] A.S. Vorobyev, A.M. Gagarski, O.A. Shcherbakov, L.A. Vaishnene, and A.L. Barabanov, JETP Letters **102**(**4**), 203 (2015).
[4] A.S. Vorobyev, A.M. Gagarski, O.A. Shcherbakov, L.A. Vaishnene, and A.L. Barabanov, JETP Letters **104**(**6**), 365 (2016).
[5] A.S. Vorobyev, A.M. Gagarski, O.A. Shcherbakov, L.A. Vaishnene, and A.L. Barabanov, JETP Letters **107**(9), 521 (2018).

[6] A.S. Vorobyev, A.M. Gagarski, O.A. Shcherbakov, and L.A. Vaishnene. In book "XXIII International Seminar on Interaction of Neutrons with Nuclei", Dubna, May 25-29, 2015. JINR, E3-2016-12, 2016, p.73.
[7] A.S. Vorobyev, A.M. Gagarski, O.A. Shcherbakov, L.A. Vaishnene. In book "XXIV International Seminar on Interaction of Neutrons with Nuclei", Dubna, May 24-27, 2016. JINR, E3-2017-8, 2017, p.343.
[8] A.S. Vorobyev, A.M. Gagarski, O.A. Shcherbakov, L.A. Vaishnene, and A.L. Barabanov. In book "XXIV International Seminar on Interaction of Neutrons with Nuclei", Dubna, May 24-27, 2016. JINR, E3-2017-8, 2017, p.413.
[9] A.S. Vorobyev, A.M. Gagarski, O.A. Shcherbakov, L.A. Vaishnene, and A.L. Barabanov. In book "XXV International Seminar on Interaction of Neutrons with Nuclei", Dubna, May 22-26, 2017. JINR, E3-2018-12, 2018, p.343.
[10]A.S. Vorobyev, A.M. Gagarski, O.A. Shcherbakov, L.A. Vaishnene, and A.L. Barabanov, Proc. of the Int. Conf. "Nuclear data for Science and Technology ND-2016", September 11-16, 2016, Bruges, Belgium. EPJ Web of Conferences **146**, 04011 (2017).
[11] R.L. Henkel and J.E. Brolley Jr, Phys. Rev. **103**, 1292 (1956).
[12] L. Blumberg, R.B. Leachman, Phys. Rev. **116**, 102 (1959).
[13] J.E. Simmons and R.L. Henkel, Phys. Rev. **120**, 198 (1960).
[14] R.B. Leachman and L. Blumberg, Phys. Rev. **137**, B814 (1965).
[15] V.G. Nesterov, G.N. Smirenkin, and D.L. Shpak, Yadernaya Fizika **4**(**5**), 993 (1966).
[16] R. H. Iyer, M. L. Sagu, in Proc. of the Nuclear Physics and Solid State Physics Symposium, Dec. 27–30, 1970; Madurai, India: Nuclear Physics, Vol. **2**, p.57 (1970).
[17] D.L. Shpak, Yu.B. Ostapenko, G.N. Smirenkin, Sov. J. of Nucl. Physics **13**, 547 (1971).
[18] Kh. D. Androsenko, G. G. Korolev, and D. L. Shpak, VANT, Ser.Yadernye Konstanty **46**(**2**), 9 (1982).
[19] J.W. Meadows and C. Budtz-Jorgensen, Proc. of the Conf. on Nuclear Data for Science and Technology, Antwerp 1982, p.740.
[20] D.L. Shpak, Yadernaya Fizika, Vol. **50(4)**, 922 (1989).
[21] V. Eismont, A. Kireev, I. Ryzhov, et al., in Proc. of the Int. Conf. on Nuclear Data for Science and Technology, May 19–24, 1997; Trieste, Italy, Conf. Proc., **59**, 658 (1997).
[22] D. L. Shpak, Physics of Atomic Nuclei, 61(8), 1333 (1998).
[23] F. Vives, F.-J. Hambsch, G. Barreau, et al., Nucl. Phys. **A662**, 63 (2000).
[24] I.V. Ryzhov, M.S. Onegin, G.A. Tutin, et al., Nucl. Phys. **A760**, 19 (2005).
[25] L.S. Leong, PhD Thesis, Universite Paris Sud, CERN-Thesis-2013-254.
[26] L.S. Leong, L. Tassan-Got, D. Tarrio, et al., Proc. of the Int. Conf. "Nuclear data for Science and Technology ND-2013", March 4-8, 2013, New York, USA. EPJ Web of Conferences **62**, 08003 (2013).
[27] D. Tarrio, L.S. Leong, L. Audouin et al., Nuclear Data Sheets, **119**, 35 (2014).
[28] E. Leal-Cidoncha, I. Duran, C. Paradela, et al., Proc. of "4th International Workshop on Nuclear Data Evaluation for Reactor applications WONDER-2015", October 5-8, 2015, Aix-en-Provence, France. EPJ Web of Conferences **111**, 10002 (2016).
[29] E. Leal-Cidoncha, et al., FIESTA 2017, LANL FIESTA Fission School & Workshop, Santa Fe, 17 -22 September 2017. https://t2.lanl.gov/fiesta2017/Talks/Leal-Cidoncha.pdf
[30] V. Kleinrath, PhD Thesis, Technischen Universitat Wien, 2015.
[31] V. Geppert-Kleinrath, F. Tovesson, J.S. Barrett, et al., arXiv:1710.00973v1 [nucl-ex] 3 Oct 2017.